Thermal Simulation of Laser Surface Modification of H13 Die Steel

Syarifah N. Aqida[1], Sumsun Naher[2], Dermot Brabazon[2]

1 Faculty of Mechanical Engineering, Universiti Malaysia Pahang, 26600 Pekan, Pahang, Malaysia

2 School of Mechanical and Manufacturing Engineering, Dublin City University, Dublin 9, Ireland

Abstract. In this study, the effects of laser parameters on the properties of glazed die steel were investigated. A Rofin DC-015 diffusion-cooled CO_2 slab laser with 10.6 µm wavelength was used. Die steel sample surfaces were prepared with a 3 µm roughness and chemically treated to improve CO_2 laser wavelength absorbance. One set of processing parameters were processed through the thermal simulation program and correlated with physical results determined from actual test samples. Set processing parameters were 1138 W peak power, 2900 Hz PRF, 24% duty cycle and 261 mm/s traverse speed. Scanning Electron Microscopy (SEM) micrographs and micro-hardness properties of the affected surface were measured. An analytical mathematical model of the heat field generated in the laser glazing process was used to predict the nominal temperature distribution in the surface and dimensions of melt pool. A thermal model using point source surface energy inputs was used to predict the thermal profiles in the die steel. This allowed estimation of the depths of microstructurally altered regions. For higher energy absorbance, the depth of the glazed surface increased from 20 µm to 40 µm. At high nominal heating to cooling rate ratios, high micro-hardness values were recorded.

Keywords: Pulse laser glazing, nominal temperature distribution, die steel, and micro-hardness.

Introduction

In high temperature metal forming, hot work tool steels are used almost exclusively to withstand the high working temperatures [1]. Hot work steels were chemically designed for toughness, good resistance to high temperature softening, high temperature oxidation resistance, and resistance to wear. In spite of these capabilities, above 600^{o}C, these dies easily wear due to thermal fatigue resulting from the high velocity of injected molten metal. Typical hardness for die casting dies is in the range of 44 to 50 HRC [2]. Continuous efforts have been reviewed on increasing die durability especially through coating and heat treatment technologies [3-6]. Most previous studies have been directed at improving the surface properties of die-casting dies to minimize heat checking, erosion, stress corrosion, and soldering [7-8].

A recent approach to achieve these goals is by use of laser surface glazing to produce a thin amorphous or nano-crystalline layer on top of the substrate [6]. In laser glazing process,

laser energy is absorbed into materials surface, the surface is melted, and the melt propagates into the bulk to a depth determined by transferred energy and material thermal properties [9]. High energy from laser beam provides a rapid heating and cooling rate on the surface which could create an amorphous structure which is harder, more resistant to heat checks and extends the dies life [7]. Glazing can be done either by pulsed or continuous mode. Previous works of Brabazon et al. focused on the surface modification of H13 die steel using continuous laser beam [10, 11]. Defects, such as porosity and bubbles occur easily with a continuous wave laser [12, 13]. The significance of pulse mode in laser glazing has not been examined in detail.

The advantage of thermal modelling of laser processing is well established. Previous researchers have implemented thermal model simulations to investigate the laser heating of surfaces and the thermal stress development at different processing parameters [14-16]. However, those studies in laser glazing have largely focused on ceramics coatings [15-17]. The main objective of this study is

to investigate the temperature distribution in laser glazed surface of AISI H13 tool steel. The temperature profile found in simulation of the glazed surface was validated experimentally. The laser glazing was done using pulse mode and parameters were varied to maximise hardness. Roughened and chemically treated samples were used to increase surface absorptivity.

Experimental

The material used in this study was H13 tool steel. Cylindrical samples with as-received 10 mm diameter were processed and analysed. Table 1 shows the chemical composition of the H13 material used as analysed using energy dispersive x-ray spectroscopy (EDXS), Inca X-Act and Microanslysis suit, Oxford Instruments. A 1.5 kW Rofin DC-015 diffusion-cooled CO_2 slab laser with 90 µm spot size and TEM_{00} mode was used. H13 samples were attached to a rotating chuck which was in turn mounted on the x-y translation stage of the laser machine [18-21]. The processing parameters were 1138 W peak power, 2900 Hz PRF, 24% duty cycle and 261 mm/s traverse speed. The spot surface traversing speed employed was calculated from rotational speed. Duty cycle affects the pulse duration which in part controls the material-beam interaction time. Samples were processed in an inert argon atmosphere. Sample surfaces were prepared with 3 µm roughness and chemically treated using Nital (2-10%) to improve CO_2 laser wavelength absorbance. The final diameter of the samples after roughening was 9.4 mm. A metallographic study of transverse sections through the processed cylindrical samples was conducted. An EVO 15 SEM and Reichart Me F2 microscope with Beuhler Omnimet Enterprise image analyser software were used for imagining purposes. Micro-hardness properties of the affected surface were measured using Leitz mini-load tester with 981 mN force.

Table 1: Chemical composition of AISI H13 die steel

Element	C	Mn	Si	Cr	Ni	Mo	V	Cu	P	S	Fe
wt %	0.32-0.45	0.20-0.50	0.80-1.20	4.75-5.50	0.30	1.10-1.75	0.80-1.20	0.25	0.03	0.03	balance

An analytical mathematical model of the heat field generated in the laser glazing process was used to predict the temperature distribution in the surface and dimensions of the resulting region of microstructure phase change or melt pool formation. The general heat conduction equation is given in Eq 1 where the sample moving at constant traverse speed, U, in x-direction. Eq. 2 gives the 3dimensional temperature distribution in glazed surface which was solved from the general heat conduction equation, previously presented by Issa et. al [22]. By taking into account the surface preparation, a 60 % surface absorbance factor was used.

$$\frac{\partial T}{\partial t} + U\frac{\partial T}{\partial x} = \alpha\left(\frac{\partial^2 T}{\partial x^2} + \frac{\partial^2 T}{\partial y^2} + \frac{\partial^2 T}{\partial z^2}\right) \quad (1)$$

$$T(x,y,z,t) = T_o + \frac{P(t)}{2\pi kr}\exp\left[i\omega t + \frac{U}{2\alpha}\left(x - r\sqrt{1+\frac{4\alpha\omega i}{U^2}}\right)\right] \quad (2)$$

where $P(t)$ is the time dependent laser power input (W), ω is the fundamental frequency of the power input (equal to 2πPRF, Hz), r is the radial distance from the power source (m), ρ is the density (kg m^{-3}), C_p is the heat capacity (J kg^{-1} $^{\circ}C^{-1}$), k is the thermal conductivity (W m^{-1} $^{\circ}C^{-1}$), and α is the thermal diffusivity of the material (m^2 s^{-1}) equal to $k/\rho C_p$. Physical and thermal properties of the H13 die steel used for the modelling are given in Table 2.

Table 2: Thermal and physical properties of H13 steels at room temperature [23].

Properties	Density	Liquidus temperature	Thermal conductivity	Specific heat	Latent heat of fusion
H13	7000 kg/m^3	1454 $^{\circ}C$	28 W/mK	447 J/kgK	2.8 x 10^5 J/kg

The temperature distribution through the modified surface depths was simulated using 'planar isotherm' software. These profiles were recorded at 20 µm depth intervals from 0 to 120 µm beneath the surface. Similar processing parameters that have been used in the processing were simulated in the software. '3D channel profile simulation' software was used to obtain temperature data at different coordinates. The temperature data was used to plot the heating and cooling rates of each point in the modified surface. A relationship between the heating/cooling rate ratio and hardness properties was then established.

In the glazing process, the H13 surface was just melted at a liquidus temperature of approximately 1454 ^{o}C and vaporisation was avoided. The significant amount of energy consumed to raise the H13 die steel to its melting temperature can be estimated. Neglecting phase change, the approximate energy required to raise the temperature and consequently to melt the surface can be calculated from heat capacity analysis (multiplying specific heat by temperature difference and by mass of material). The amount of heat required to reach the melting temperature is thereby approximated as 640,104 J/kg. In this software, no heat losses through radiation and convection were considered.

Results and Discussion

Figure 1 shows the cross section of the modified surface of sample F13 in the Y and Z axis. The dimension of the melted region, which is required for surface modification to occur, was limited by the volume of material for which the energy provided could raise the metal temperature to the material melt temperature, 1454$^{\circ}C$. The region where the temperature was raised to the melt

temperature was approximately 49 µm deep. As the simulation considered constant thermal properties of H13 steel throughout the process and neglected latent heat, the glazed layer shown by simulation was approximately twice as deep compared to that seen in the experimental results.

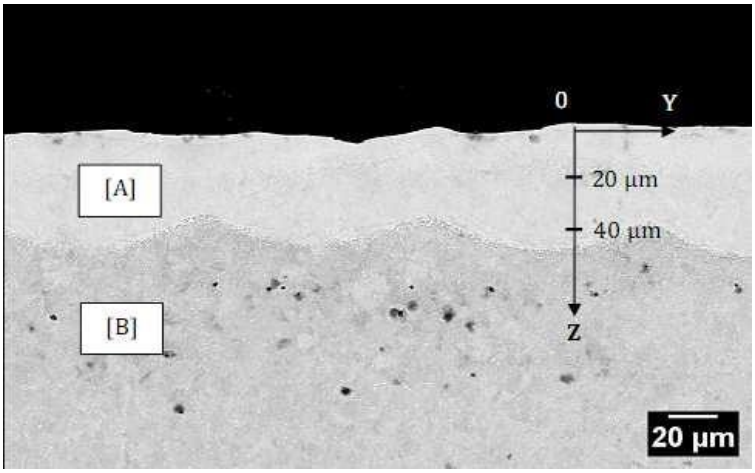

Figure 1: Modified layer [A] formed on substrate [B] after laser surface modification.

In Figure 2, the thermal model simulation indicates as expected reducing temperature for each Z (depth) plane upon progressing further into the substrate. Referring to Figure 2 (a) and (b), when the thermal model was simulated at Z=40 µm or less, the maximum temperature achieved is represented at a nominal value of 1.

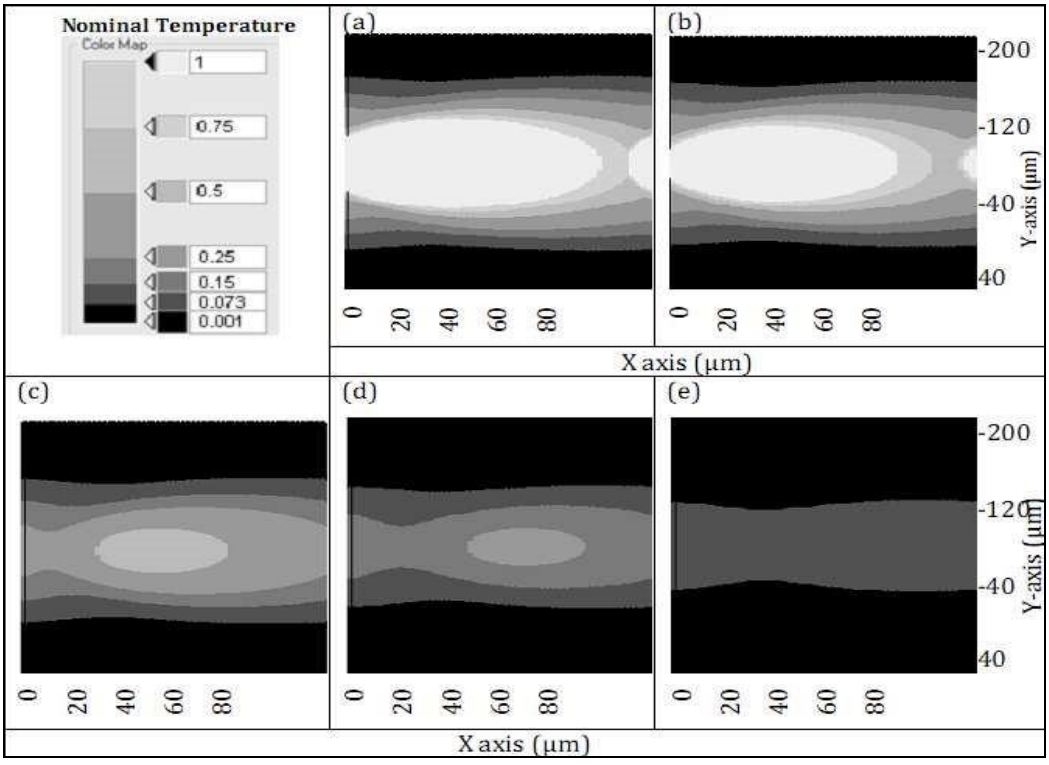

Figure 2: Nominal temperature distribution simulation in glazed surface of H13 along depth, at (a) Z=20 µm, (b) Z=40 µm, (c) Z=80 µm, (d) Z=100 µm and (e) Z=120 µm.

At 80 µm depth, the maximum nominal temperature achieved was 0.62 as shown in Figure 2(c). In Fig. 2(d) and (e), the maximum nominal temperatures of 0.28 and 0.13 were recorded at 100 µm and 120 µm deep respectively. The temperature distribution plots from simulation allowed for the heating and cooling rates of any particular point within the glazed surface to be calculated. Heating and cooling rates are significant values in laser glazing in order to control the size of the microstructurally altered region after solidification.

Heating and cooling profiles from the model are shown in Figure 3. In Figure 3, the nominal temperature as a function of time was modelled for the H13 sample processed at 1138 W power, 24% duty cycle, and 261 mm/s traverse speed. At 2900 Hz, the time needed for a complete pulse was 0.35 ms. At a specific point of Y= 70.6 µm, the nominal temperature distribution along the molten pool depth was plotted. The time needed to reach the maximum nominal temperature at the surface (where Z = 0), was 0.121 ms. The initial and maximum temperature achieved decreased with increasing depth. The time duration to reach these temperatures at deeper Z positions was also longer relative to shallower regions. Cooling rates recorded at the centre of the melt pool were twenty times higher than the cooling rate at a distance of 100 µm from the centre in Y direction, for six Z positions (0, 20, 40, 60, 80 and 100 µm).

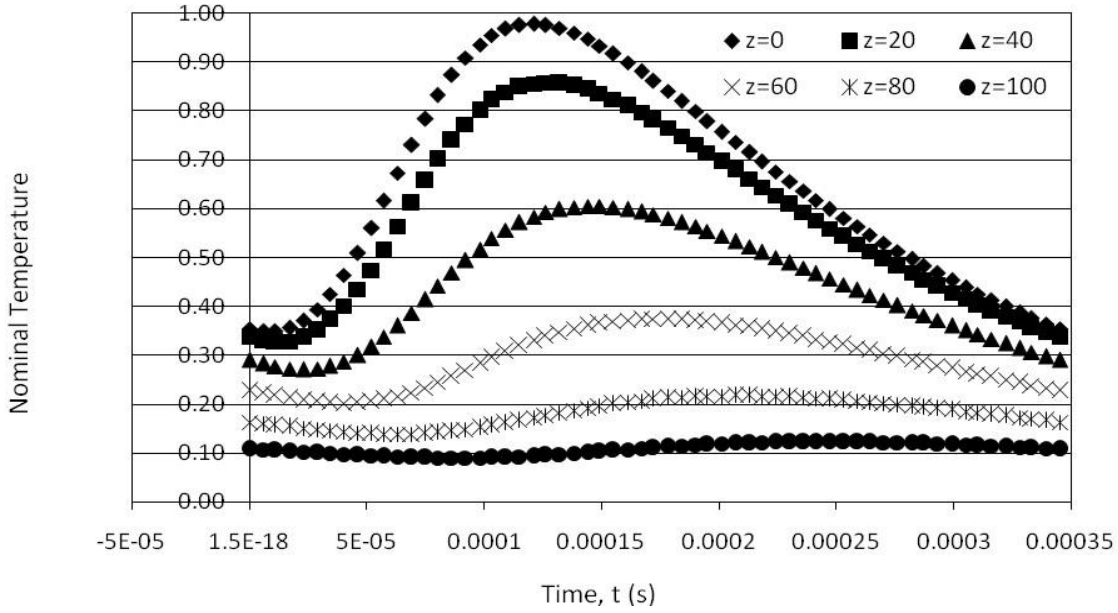

Figure 3: Nominal temperature as a function of time (at Y=70.6 µm).

The simulation of temperature profile in the modified surface was indirectly examined experimentally. The micro-hardness values measured at different distances within the processed surface are presented in Figure 4. The maximum hardness of 824 $HV_{0.1}$ resulted from 2377 s^{-1} nominal cooling rate and 4618 s^{-1} nominal heating rate, at a 20 µm modified surface depth.

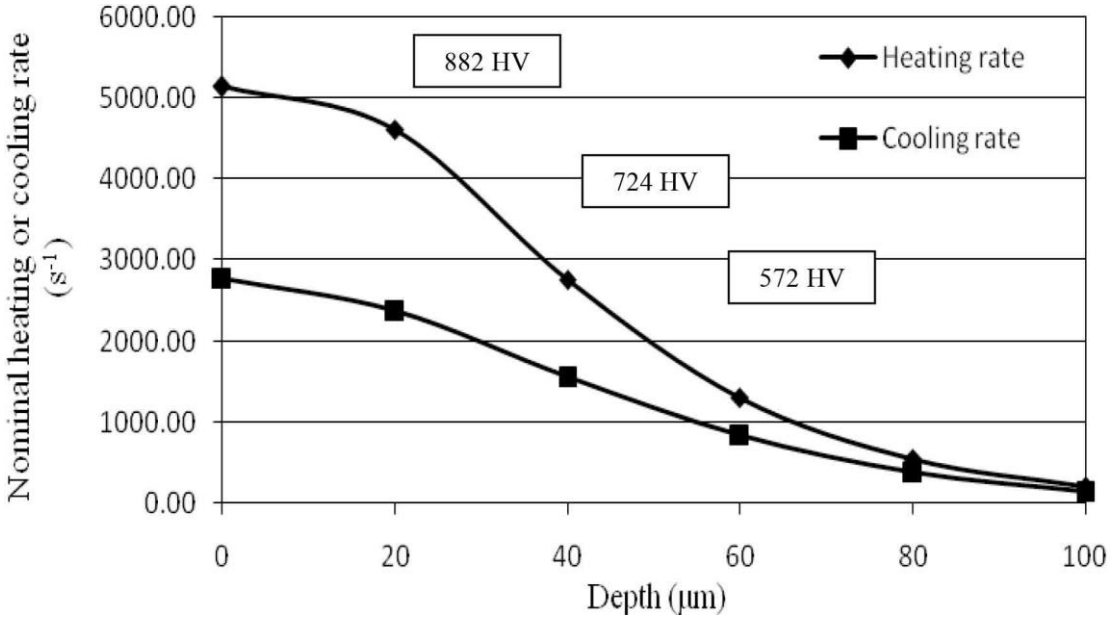

Figure 4: Micro-hardness of glazed surface corresponding to nominal heating and cooling rate of molten pool in the glazed surface along the depths.

At 724 and 572 HV0.1 micro-hardness, the nominal heating to cooling rate ratio was 1.76 and 1.54 respectively. As the heating to cooling rate ratio decreased, the micro-hardness also decreased.

Conclusion

The results from thermal modelling, metallography and micro-hardness measurement have been analysed to provide a new insight into the processing-properties relationships in the laser glazing of die steels. Increasing surface roughness to 3 µm improved the pulse energy absorbance which consequently increased the molten region width and depth. The simulations of temperature distribution in pulse laser glazed surface can predict the heating and cooling rate at specific points in the molten pool. By evaluating these thermal rates, the hardness of the processed samples can be predicted. The maximum hardness of 882 $HV_{0.1}$ was achieved at nominal heating to cooling rate ratio of 1.94. At higher Z values, lower heating and cooling rates occurred with corresponding reductions in the micro-hardness. These findings are important for the fundamental understanding of the process and the provision of surface modification process maps for use with the pulse laser beam glazing process.

Acknowledgement

The authors would like to acknowledge the support from Dublin City University and the Ministry of Higher Education, Malaysia for funding this work.

References

[1] H. Coldwell, R. Woods, M. Paul, P. Koshy, R. Dewes, and D. Aspinwall, J. Mater. Process. Technol. 135 (2003) 301–311.

[2] H.Yan, J. Hua and R. Shivpuri, Mater. Des. 28 (2007) 272–277.

[3] S. V. Shah and N.B. Dahotre, J. Mater. Process. Technol. 124 (2002) 105–112.

[4] J. Tušek, B. Taljat and D. Klobcar, Metalurgija, 46 (2007) 67-71.

[5] R.J. DiMelfi, P.G. Sanders, B. Hunter, J.A. Eastman, K.J. Sawley, K.H. Leong, J.M. Kramer, Surf. Coat. Technol. 106 (1998) 30-43.

[6] W. Jiang and P. Molian, Surf. Coat. Technol. 135 (2001) 139-149.

[7] Y. Sun, S. Hanaki, M. Yamashita, H. Uchida and H. Tsujii, Vacuum 73 (2004) 655–660.

[8] C. Mitterer, F. Holler, F. Ustel and D. Heim, Surf. Coat. Technol. 125 (2000) 233-239.

[9] S. H. Aldajah, O. O. Ajayi, G. R. Fenske and Z. Xu J. Tribol. 127 (2005) 596-604.

[10] D. Brabazon, S. Naher and P. Biggs, Solid State Phenom. 141-143 (2008) 255-260.

[11] D. Brabazon, S. Naher and P. Biggs, Int. J. Mater. Form. 1 (2008) 985–988.

[12] A.J. Pinkerton, L. Li, Appl. Surf. Sci. 208-209 (2003) 405-410.

[13] H.L. Tsai and P.C. Tsai, Surf. Coat. Technol. 71 (1995) 53-59.

[14] B.S. Yilbas, A.F.M. Arif, C. Karatas and M. Ahsan, Appl. Surf. Sci. 253 (2007) 5544–5552.

[15] J.F. Li, L. Li and F.H. Stott, Acta Mater. 52 (2004) 4385–4398.

[16] J. Singh, B.N. Bhat, R. Poorman, A. Kar and J. Mazumder, Surf. Coat. Tech. 79 (1996) 35-49.

[17] A.A. Peligrad, E. Zhou, D. Morton and L. Li, Opt. Laser Technol. 33 (2001) 7-13.

[18] S. N. Aqida, F. Calosso, D. Brabazon, S. Naher and M. Rosso, Int. J Mater Form, Vol. 3 Suppl 1:797-800, 2010.

[19] S. N. Aqida, M. Maurel, D. Brabazon, S. Naher, and M. Rosso, Int. J Mater Form, Vol. 2 Suppl 1:761-764, 2009.

[20] E Chikarakara, S Naher and D Brabazon, accepted to: Surf and Coat. Tech. (2011).

[21] E. Chikarakara, S. Naher and D. Brabazon: Appl. Phys. A, 101, 2, 2010

[22] A. Issa, D. Brabazon and M.S.J. Hashmi, J. Mater. Process. Technol. 207 (2008) 307–314.

[23] Y. Lin, K. M. McHugh, Y. Zhoua and E. J. Lavernia, Scr. Mater. 55 (2006) 581–584.